Hindawi
Journal of Chemistry
Volume 2018, Article ID 9813827, 12 pages
https://doi.org/10.1155/2018/9813827

Research Article

Fabrication of Bilayer Coating of Poly (3,4-ethylenedioxythiophene)-Halloysite/Chitosan and Mg^{2+}/Sr^{2+}-Doped HAP on Titanium Alloy for Biomedical Implant Applications: Physicochemical and *In Vitro* Biological Performances Studies

Manickam Chozhanathmisra,[1] Dharman Govindaraj,[2] Palanisamy Karthikeyan,[3] Kannaiyan Pandian,[4] Liviu Mitu,[5] and Rangappan Rajavel[1]

[1]*Department of Chemistry, Periyar University, Salem 636 011, Tamilnadu, India*
[2]*Biomaterials in Medicinal Chemistry Lab, Department of Natural Products Chemistry, School of Chemistry, Madurai Kamaraj University, Madurai 625021, India*
[3]*Department of Chemistry, Periyar University Constituent College of Arts and Science Idappadi, Salem 637 102, Tamilnadu, India*
[4]*Department of Inorganic Chemistry, University of Madras, Guindy Campus, Chennai 600025, Tamilnadu, India*
[5]*Department of Physics & Chemistry, University of Pitesti, Pitesti 110040, Romania*

Correspondence should be addressed to Liviu Mitu; ktm7ro@yahoo.com and Rangappan Rajavel; drrajavelpu@gmail.com

Received 25 May 2018; Revised 10 July 2018; Accepted 16 July 2018; Published 18 September 2018

Academic Editor: Jean-Marie Nedelec

The prime objective of the present work is to develop biocompatible overlayer-deposited titanium alloys to replace already available titanium alloy-based biomaterials for implantation applications. Here, we prefer to use a bilayer coating on titanium alloys instead of single coating. The adhesion and biocompatibility of titanium alloy is improved by coating with a bilayer, for example, PEDOT-HNT/CS-MHA composite using the electrochemical deposition method. Corrosion behavior of the PEDOT-HNT/CS-MHA bilayer composite coating was investigated in the PBS medium by polarization studies. The functional groups, phase purity, surface morphology, and wettability of the PEDOT-HNT/CS-MHA were characterized by various instrumental techniques like FTIR, XRD, SEM, and contact angle techniques. From the above studies, it is proved that PEDOT-HNT/CS-MHA-coated Ti alloy showing a better biocompatibility and corrosion resistance than the PEDOT-HNT-deposited Ti alloy. In addition, the *in vitro* bactericidal and cell viability studies were also carried out to further confirm the biocompatibility of the protective coating. Hence, the bilayer deposition has shown excellent stability and biocompatibility and can be used for the potential biomaterials for orthopedics applications.

1. Introduction

Recent days, scientists and researchers have shown interest on preparing new biomaterials to discover a new solution for improving treatment for different bone-related diseases and injuries [1]. Titanium (Ti) and its alloys are the possible options for the load-bearing implant material especially used in bone tissue applications [2]. But the Ti alloy demonstrates poor integration to bone tissues and a challenge for bacterial infections [3, 4]. So, surface modification is necessary for improving the biological properties like improving the surface morphology, corrosion property, cell adhesion, cytoskeleton organization, antibacterial activity, and osteogenesis property [5]. In order to achieve the above vital properties of Ti alloys, coating them with appropriate materials is necessary. Hydroxyapatite ($Ca_{10}(PO_4)_6(OH)_2$)

(HA) has favorable bioactive properties making it a preferred biomaterial for both orthopedic and dental applications [6]. Chemical composition of HA is similar to natural human bone mineral, that can improve osteoconductivity and osteointegration of surrounding tissues, leading to its ingrowths of a newly formed bone on protective coatings [7]. HA-based biomaterial had some drawback of slow cell growth rate and poor mechanical properties during implant surgery and is also susceptible to bacterial activity. In order to overcome this problem, HA has been substituted with different mineral ions which have multiple important functions in biological systems [8]. It is reported that the incorporation of Mg^{2+} or Sr^{2+} into the hydroxyapatite coatings improves the formation of osteoblast and osteoclast activity and thus improves the bone growth of the apatite layer on the surface of the coating in simulated body fluid (SBF). These cations are beneficial for tissue growth, leading to potential applications in bone repair and substitution for orthopedic and dental applications [9, 10].

Biocompatible polymeric materials like poly(3,4-ethylenedioxythiophene), PEDOT, is a stable conductive polymer and widely used for biomedical implant applications [11] due to their similar structural feature like melanin. The PEDOT has high conductivity with greater environmental stability, and its coatings are relatively soft and nonbiodegradable when it is introduced in the implantable material [12]; PEDOT composite coating exhibited anticorrosion protection behavior with improved cell growth on the MG-63 osteoblast cell. However, metal dissolution on metallic materials before monomer oxidation is the major obstacle which prevents adherent and uniform film formation on the surface using electrodeposition of conducting polymers. To overcome these problems implant materials should be treated, which facilitates the electrodeposition process [13, 14].

Similarly, chitosan (CS) is an interesting biopolymer, which has good antimicrobial, biocompatible, and biodegradable features [15] due to its excellent film-forming properties and is easy for functionalization. Recently, CS has been extensively used for a number of applications such as cosmetic and metal-based biomaterials which are applied to bone grafts and scaffolds for tissue engineering. However, low mechanical properties of CS can be improved by modification. CS incorporation of inorganic materials can improve the mechanical properties of composites. It is also used as a binder or as glue to prepare HA-based biomaterials [16, 17].

Halloysite nanotube ($Al_2Si_2O_5(OH)_4{\cdot}2H_2O$) (HNT) is a naturally occurring clay mineral with a nanotubular-layered structure which is widely used for drug delivery, fillers in polymer nanocomposite, electrochemical and sensor applications, and corrosion-resistant coating [18]. Applicable properties are tunable surface chemistry, high hydrophilicity and mechanical strength, superdispersion and sustained releases, and biocompatibility [19]. It is also an alternative to replace the expensive carbon nanotube (CNTs) [20]. HNTs are also nontoxic for cells which are used for the fabrication of biocompatibility protective coating for various biomedical applications [21]. Recently, Aburto et al. reported that the HNT/PEDOT improves thermal stability and electrical conductivity of PEDOT and proposed a high surface area to volume ratio of the composite passive layer for protective coating [22].

The major challenge of coating the alkali-treated Ti alloy surface with PEDOT-HNT/CS-MHA nanocomposite is an important task to overcome the above said problems. A composite material is generally coated on metal substrates using different types of coating methods. There are several advantages of using electrodeposition coating because the composite coated on alkali-treated Ti alloy substrate enhances the bonding rate of implants to human bones and bond strength. Hence, there is an urgent need to estabilise a novel orthopedic implant material with cheaper cost and with a better adhesive layer and biocompatibility [23–25]. Recently, we have shown that the copolymers of PEDOT and their halloysite Zn-HNT composites are excellent corrosion protective coatings [26] for implant applications with greater biocompatibility. In the present work, novel PEDOT-HNT/CS-MHA bilayer composite coatings were produced on alkali-treated Ti alloy substrates by means of the electrodeposition process. The influence of PEDOT-HNT/CS-MHA coating on Ti alloys on biological aspect as well as corrosive properties of the coatings was investigated.

2. Materials and Methods

2.1. Materials. The chemicals used for the preparation of PEDOT-HNT and CS-MHA were obtained from commercial sources. The ethylenedioxythiophene, chitosan, calcium chloride dihydrate ($CaCl_2{\cdot}2H_2O$), strontium nitrate hexahydrate ($Sr(NO_3)_2{\cdot}6H_2O$), magnesium chloride hexahydrate ($MgCl_2{\cdot}6H_2O$), diammonium hydrogen phosphate ($(NH_4)_2HPO_4$), acetone, acetonitrile, lithium perchlorate, ethanol, hydrochloric acid (HCL), and ammonium hydroxide (NH_4OH) were purchased from Sigma-Aldrich, India. All analytical grade reagents were used without any further purification, double distilled water was employed as the solvent throughout the electrodeposition, and other experiments were performed at room temperature. All other reagents were of analytical grade and used without any further purification.

2.2. Preparation of Ti Alloy Specimens. The Ti alloy used in this study was cut into $10 \times 10 \times 3\,mm^3$. These metal substrates were then mechanically ground with 400–1500 grade abrasive silicon carbide paper and ultrasonically cleaned for 10 min in absolute ethanol and acetone, and finally, the metal substrate (working electrode) was alkali treated and used as surfaces for electrodeposition. Then, it is dried in air and used for further experiments.

2.3. MHA Electrolyte Preparation. Different compositions of HA with two different dopants like Mg and Sr were prepared by mixing a required amount of metal salts with ammonium dihydrogen phosphate, and the resulting solution was maintained at a pH value of 4.5 in each electrolyte, which was adjusted using nitric acid (HNO_3) and sulphuric acid

(H_2SO_4). The electrochemical deposited the HA-Ti alloy, and the Ti-6Al-4V alloy samples were collected after cleaning with distilled water and then dried at 50°C in a vacuum chamber overnight.

2.4. EDOT, HNT, and Chitosan Electrolyte Preparation. The chemical 3,4-ethylenedioxythiophene (EDOT) was purchased from Sigma-Aldrich. The electrolyte solution was prepared with 1 g of EDOT dissolved in 0.1 M lithium perchloride in acetonitrile solution in a 100 ml standard measuring flask. The solution was cooled to room temperature and stored at 4°C. Halloysite clay in 0.1 M was dispersed in double distilled water by ultrasonication for 30 minutes. Chitosan powder (1.0% w/v) was dissolved in acetic acid (1.0% v/v), and the pH was adjusted to 5.5. Then, it was filtered to remove the undisclosed particles.

2.5. Composite Coating on Ti Alloy by Electrodeposition Method. Electrochemical polymerization of EDOT on the HNT-modified alkali-treated Ti alloy was done in a three-electrode cell arrangement using cyclic voltammetry (CV CHI 760C electrochemical workstation (USA)) in which the alkali-treated Ti alloy and platinum electrodes were the working electrode and counterelectrode, and saturated calomel electrode (SCE) served as the reference electrode, respectively. The electrodeposition of ethylenedioxythiophene on the alkali-treated Ti alloy was achieved in 0.5 M $LiClO_4$ solution containing 0.1 M PEDOT. The applied potential was scanned between +1.4 and −0.8 V versus SCE for 20 cycles at a fixed scan rate of 20 mV/s [26].

2.6. Electrochemical Investigation of Composite-Modified Ti Alloys. The electrochemical behavior of the PEDOT-HNT, PEDOT-HNT/CS-HA, and PEDOT-HNT/CS-MHA composite-deposited alkali-treated Ti alloy was characterized by potentiodynamic polarization and electrochemical impedance spectroscopy measurements (EIS) in stimulated body fluid (SBF) solution. The electrochemical studies were performed in a conventional three-electrode cell. Alkali-treated Ti alloy was used as the working electrode, and the saturated calomel electrode (SCE) and platinum electrode were taken as the reference and counterelectrodes, respectively; for all measurements, pH of the electrolyte was maintained at 4.5, and the temperature was kept at 37°C. Potentiodynamic polarization studies were carried out at a scan rate of 1 mVs^{-1} in the prospective range between −0.8 and +0.2 V. The electrochemical impedance spectroscopy (EIS) measurements were performed in the frequency range of 10 MHz to 100 kHz with the perturbation amplitude of 5 mV. All plots were made by commercial software, and each experiment was repeated five times to check the reproducibility of implant surface [26].

2.7. Physicochemical Characterization. The Fourier transform infrared (FTIR) analysis of the PEDOT-HNT, PEDOT-HNT/CS-HA, and PEDOT-HNT/CS-MHA composite coating was performed to identify the functional groups using PerkinElmer FTIR spectroscopy. Coated samples were analyzed in the wavenumber range 400–4000 cm^{-1} at a resolution of 4 cm^{-1}, using the KBr pellet technique. The compositions of the PEDOT-HNT, PEDOT-HNT/CS-HA, and PEDOT-HNT/CS-MHA composite coatings on alkali-treated Ti alloy substrates were analyzed by X-ray diffraction (Shimadzu XRD-6000) using Cu Kα radiation scanning from the 2θ range between 20° and 80° angles with a scanning speed of 10 min^{-1}. After XRD peak positions were compared with JCPDS files, the phases on coatings of the implant surface can be determined. The surface morphology of various composite coatings was observed with a high-resolution scanning electron microscopy (HRSEM). Prior to observation, the composite coatings were sputtered with gold for better conductivity. The contact angle measurement was carried out to investigate the surface wettability of the samples by using a sessile drop goniometer. The water drop deposited on the implant surface, under gravity, has a tendency to spread until the cohesion (internal forces) of the doubly distilled water occurs; hence, the capillary (surface tension) forces are in balance, under gravity forces, and an equilibrium state is reached. The camera was positioned to finally determine the hydrophobic or hydrophilic nature of the implant surfaces. An equal volume of distilled water was placed on every sample, and all the measurements were taken at room temperature. Distilled water and hexadecane were used as a liquid sample to study the residing angle of the droplets.

2.8. Antibacterial Assay. The antibacterial property of the PEDOT-HNT/CS-MHA composite were evaluated by Gram-positive (*Staphylococcus aureus*) and Gram-negative bacteria (*Escherichia coli*) by the agar well method. The media of the plates consisting agar nutrient broth were prepared, and wells were made in the plate. All plates were streaked with bacteria (100 μL, 104 CFU) and spread evenly on the plate. After 20 min, the wells were packed with various concentrations of the samples such as 20 μL, 40 μL, 60 μL, and 80 μL. The distilled water was used as the negative control. All the plates were incubated at 37°C for 24 h, and the diameters of the inhibition zones were noted. The assay was repeated twice, and the mean of the three experiments was recorded.

2.9. Cell Culture. The MG-63 cells were purchased from the National Centre for Cell Science (Pune, India). The PEDOT-HNT/CS-MHA composite was immersed in 75% ethanol for 3 h and then repeatedly rinsed with phosphate buffer solution (PBS) to remove residual ethanol. The cells were cultured in the α-MEM medium consisting 10% PBS and 100 $U{\cdot}ml^{-1}$ penicillin-streptomycin antibiotics at 37°C in a 5% CO_2 incubator. The media were changed twice weekly. The cell proliferation was measured using the CCK-8 assay kit. The cells were seeded with the PEDOT-HNT/CS-MHA composite, and the cells were cultured at 37°C in a 5% CO_2 incubator for 1, 3, and 7 days. CCK-8 solution (10 μL) was subsequently added to each well and incubated for 3 h in an incubator. The absorbance of each well was measured using a microplate absorbance reader (Model 680; Bio-Rad,

Hercules, CA, USA) at 450 nm. All experiments were performed in triplicate, and their average values are used for further analysis.

3. Results and Discussion

3.1. Electrochemical Deposition of PEDOT-HNT Composites. The electrochemical deposition method was carried out to deposition a uniform coating of PEDOT on both HNT as well as CS-MHA-modified Ti alloys. Figure 1 shows cyclic voltammetry behavior of continuous cycling between the preselected potential ranges by placing Ti alloy substrates in electrolyte solution consisting of a stable dispersion of 0.1 M $LiClO_4$ containing 0.1 M EDOT and HNT. The electrodeposition was performed by potential cycling between +1.4 and −0.6 V versus SCE. Inner layers successively deposited onto the Ti alloy substrates act as an electrical insulator of undesirable leakage. Before experiment, the coated samples were stabilized at their OCP. Furthermore, the outside layer of HA composite was coated in the galvanostat mode. Successively, CS-HA and CS-MHA composites were electrodeposited on the coating by chronoamperometry.

3.2. FTIR Spectra. For the qualitative confirmation of the PEDOT-HNT, CS-MHA, and PEDOT-HNT/CS-MHA, bilayer coated on the alkali-treated Ti alloy substrate was analyzed using FTIR spectroscopy (Figure 2). The FTIR spectrum of PEDOT-HNT (a) possessed exclusively the absorption bands characteristic for PEDOT and HNT. Figure 2(a) shows the FTIR spectrum of PEDOT, and the vibrations around 1385 cm^{-1} are due to the C-C stretching of the thiophene ring. The vibrations at 1208 cm^{-1} and 1120 cm^{-1} originate from stretching of the C-O-C bond in the ethylenedioxy group and ClO_4^- ion dopants from the supporting electrolyte, respectively [26]. Furthermore, the absorption band of 873 cm^{-1} is assigned to the vibrational band of the C-S bond in the thiophene ring. Thus, the HNT-derived band at 988 cm^{-1} and 1067 cm^{-1} are attributed to the Al-O and O-Si-O stretching vibrations, respectively. In addition, the bands at 527 and 793 cm^{-1} are due to the vibrations of Al-O-Si and Si-O-Si, respectively [26]. Figure 2(b) shows the 1062 cm^{-1} absorption band was ascribed to PO_4^{3-} ($\nu 3$) stretching vibrations and the 575, 620 cm^{-1} absorption bands to PO_4^{3-} ($\nu 3$) bending vibration ($\nu 4$) in the composite of the HA phase. The 986 cm^{-1} and 1062 cm^{-1} peaks were assigned to the symmetric stretching ($\nu 1$) at the PO_4^{3-} of the P-O bond [7, 25]. The most characteristic bands of CS were visible at 1650 cm^{-1} and 1554 cm^{-1}, which were assigned to the amide bond of CO-NHR, and the protonated amine groups of NH_3^+ are deformation vibrations, while the band located at 1385 cm^{-1} correspond to the C-H bonds on the CS. Also, the presence of bands in the range of 1136 cm^{-1} can be assigned to the C-O stretching vibrations in the CS chain [15]. According to the FTIR results shown in Figure 2(c), the position and the intensity of PEDOT-HNT peaks change in PEDOT-HNT/CS-HA coating and shifted to lower wavenumbers [15]. This behavior proves the PEDOT-NT/CS-MHA electrolyte in the form of a bilayer coating on alkali-treated Ti alloy substrate.

3.3. XRD Analysis. Figures 3(a)–3(c) illustrate the results of XRD characterizations of PEDOT-HNT, CS-MHA, and PEDOT-HNT/CS-MHA bilayer composites coatings on the alkali-treated Ti alloy substrate. Figure 3(a) illustrates the 2 theta values of PEDOT with two peaks at 12.5° and 26°. The diffractogram of PEDOT-HNT confirms the presence of PEDOT. In addition to the characteristic peaks of HNT, the two reflections detected at 20° and 24° originate from the PEDOT-HNT composite, and another peak showed 35° and 62° (JCPDS file no 29–1487). Figure 3(b) shows the XRD patterns of CS-MHA. The most intense peaks, observed at 25°, 29°, 30°, 31°, 32°, 49°, and 51°, originate from apatite. In accordance with the literature (JCPDS file No. 09–432) and our previous studies [7], the so-obtained MHA diffractogram indicates a poorly crystalline, non-stoichiometric form due to mineral ions substituted in MHA crystal sites. The CS composite was in a crystalline state with two main diffraction peaks at about 11.6° and 20.2°, which was coated on the alkali-treated Ti alloy substrate (Figure 3(c)) [15]. Thus, all these peaks demonstrate that the bilayer composite coating contains both CS-MHA and PEDOT-HNT. Hence, the PEDOT-HNT/CS-MHA bilayer composite coating has nominal lattice distribution. Also, no intercalation can be observed for the PEDOT-HNT/CS-MHA bilayer coated composite.

3.4. Morphological and Elemental Investigations. HRSEM micrographs of the PEDOT-HNT coated, CS-MHA coated, and PEDOT-HNT/CS-MHA coated on alkali-treated Ti alloy are shown in Figures 4(a)–4(c). The surface morphology of the HNT-PEDOT-coated Ti alloy shown in Figure 4(a) exhibited the formation of flake-like structure and uniform microstructure. The surface morphologies of the electrodeposition of CS-MHA on the PEDOT-HNT-coated alkali-treated Ti alloy shown in Figure 4(b) clearly depict that all the coatings possess a uniform spherical network structure. It is revealed that the presence of minerals does not affect the morphology of the coated layer appreciably. It is interesting to note that the most of the pores are interconnected which can be favorable to the growing bone [25]. The interconnected pores can allow the attachment and proliferation of diverse cell types responsible for the formation of tissues on PEDOT-HNT/CS-MHA-coated alkali-treated Ti alloy substrates, which can be uniformly dispersed within or on the composite coatings (Figures 4(a)–4(c)), as confirmed by element maps (Figures 4(a)–4(c)). The cross-sectional surface morphology of the bilayer composite coating was illustrated in Figure 4(d). The composite-like PEDOT-HNT layer possessed the thickness of ~26 μm and that of the bilayer composite-like CS-MHA was ~21 μm. Surprisingly, the interface among the flake-like PEDOT-HNT layer and spherical-like CS-MHA layer exhibited good adhesion without any defect. Thus, good initial stage protection for the alkali-treated Ti alloy is expected. The elemental mapping of the coated materials by

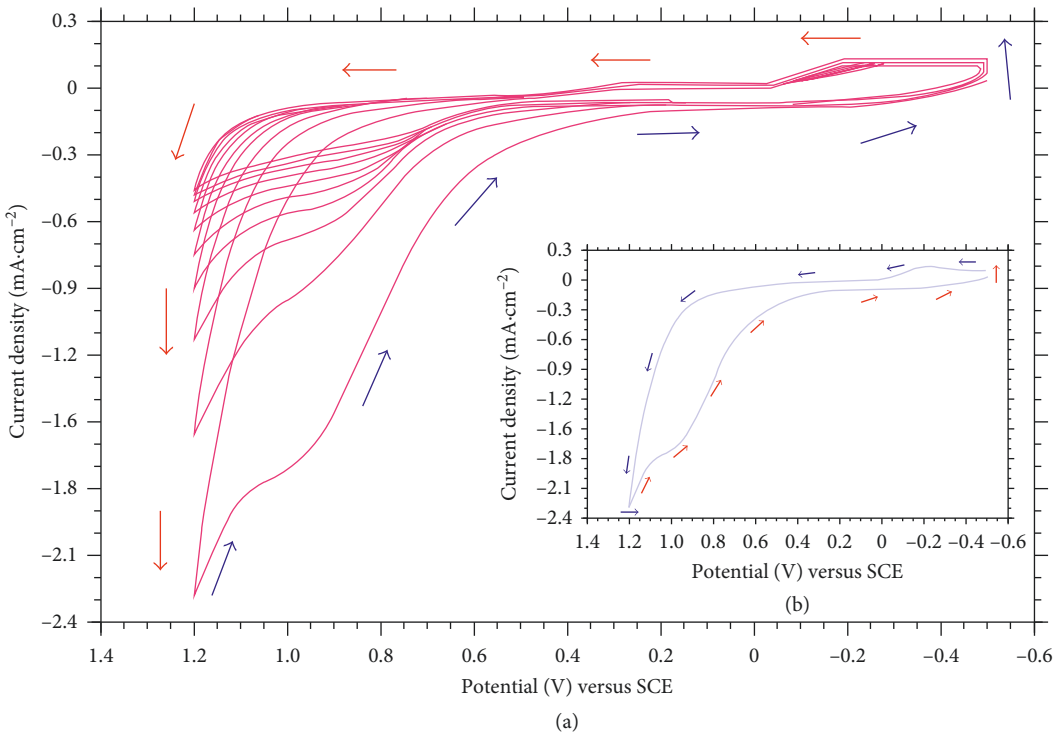

Figure 1: Cyclic voltammograms for the PEDOT-HNT composite coating on alkali-treated Ti alloy substrates for cycle numbers 1–20 at a scan rate of 50 mV·s^{-1}.

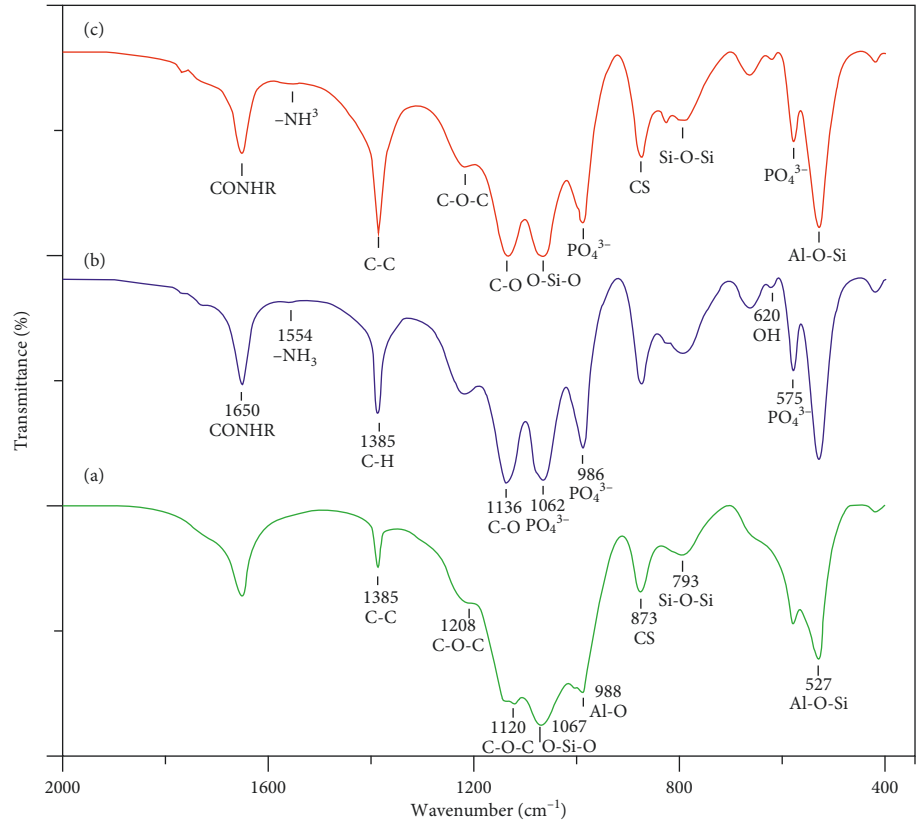

Figure 2: FTIR spectra of (a) PEDOT-HNT, (b) CS-MHA, and (c) PEDOT-HNT/CS-MHA bilayer composite coatings.

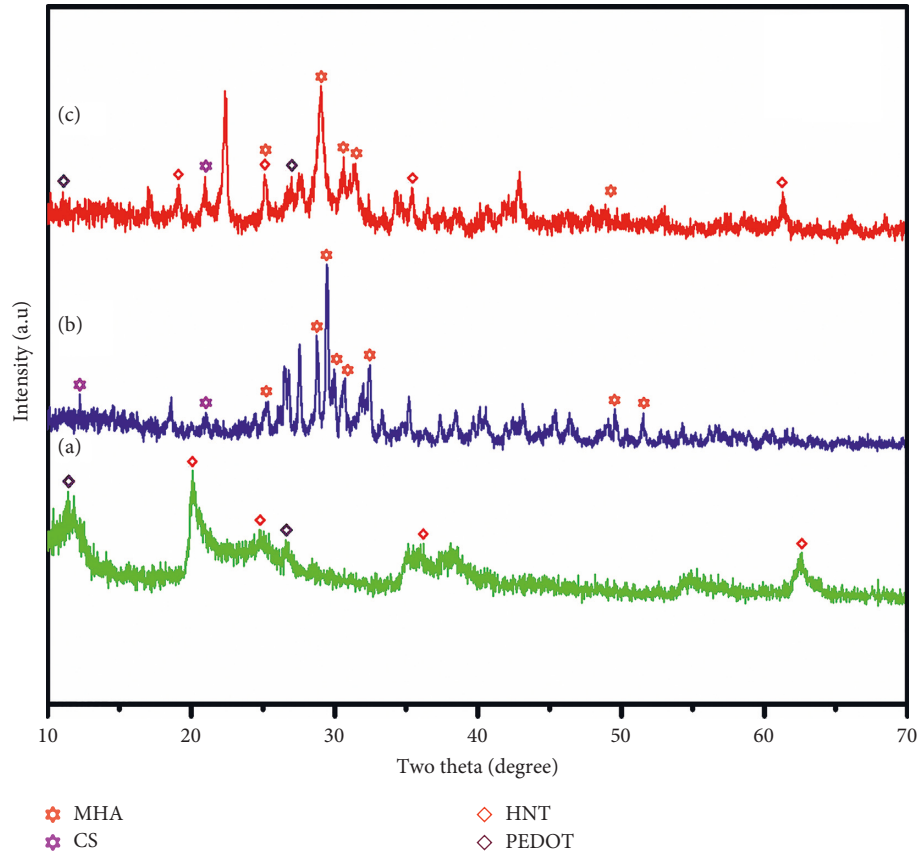

Figure 3: XRD patterns of (a) PEDOT-HNT, (b) CS-MHA, and (c) PEDOT-HNT/CS-MHA bilayer composite coatings.

EDS shows the uniform deposition of different elements like Ca, P, Sr, Mg, Al, Si, C, O, N, and S at the composite coatings on substrates site (Figure 4(e)).

3.5. Electrochemical Characterization

3.5.1. Potentiodynamic Polarization Studies. Polarization curves of alkali-treated Ti alloy substrates and PEDOT-HNT, PEDOT-HNT/CS-HA, and PEDOT-HNT/CS-MHA composite-coated Ti alloy substrates are exhibited in Figure 5. To determine the polarization tests, scanning of a potentiality lower open-circuit potential (OCP) values were conducted. Corrosion parameters such as corrosion potential (E_{corr}) and corrosion current density (i_{corr}) which were obtained from polarization curves using Tafel extrapolation are illustrated in Figure 5(a). When polarization curves were investigated, the uncoated Ti alloy specimen substrates displayed a corrosion potential (E_{corr}) of −0.5429 V, and both coated samples remarkably improved the corrosion resistance. The E_{corr} values for PEDOT-HNT, PEDOT-HNT/CS-HA, and PEDOT-HNT/CS-MHA coatings were estimated as −0.4072 V, −0.1568 V, and −0.1248 V, respectively. The positive shifting of E_{corr} evidently showed an increase in the corrosion resistance of the composite-coated specimen's substrate, thereby indicating that the Ti alloy has favorable corrosion resistance with the inside of the PEDOT-HNT/CS-MHA. i_{corr}, which is proportional to the corrosion rate, is another significant parameter in determining the corrosion characteristic of the specimens. i_{corr} of PEDOT-HNT, PEDOT-HNT/CS-HA, and PEDOT-HNT/CS-MHA composite coatings was determined as $-5.2107\,\mu A{\cdot}cm^{-2}$, $-6.2527\,\mu A{\cdot}cm^{-2}$, and $-6.3504\,\mu A{\cdot}cm^{-2}$, respectively, whereas the i_{corr} value for the alkali-treated Ti alloy specimen was determined as $-5.0315\,\mu A{\cdot}cm^{-2}$. The corrosion current densities were obviously reduced when the corrosion potential values moved in the cathodic direction to higher values. It could be noticed that the PEDOT-HNT coating between the Ti alloy surface and CS-HA coating acts as a corrosion protection barrier, thereby preventing the deterioration of the metal.

3.6. Electrochemical Impedance Spectroscopy Studies. The electrochemical impedance spectra in the form of Nyquist plots for the alkali-treated Ti alloy, PEDOT-HNT, PEDOT-HNT/CS-HA, and PEDOT-HNT/CS-MHA composite-coated Ti alloy specimens in SBF solution at an OCP condition are shown in Figure 5(b). The Rp value obtained for the PEDOT-HNT-coated Ti alloy was found to be greater ($5.228 \times 10^6\,\Omega{\cdot}cm^2$) than that of the alkali-treated Ti alloy ($1.431 \times 10^5\,\Omega{\cdot}cm^2$) specimen. This is attributed to the effective protection of the Ti alloy by the PEDOT coating. As seen from Figure 5(b), the Rp value for bilayer PEDOT-HNT/CS-HA and PEDOT-HNT/CS-MHA-coated Ti alloy was found to be $8.896 \times 10^6\,\Omega{\cdot}cm^2$ and $9.517 \times 10^6\,\Omega{\cdot}cm^2$

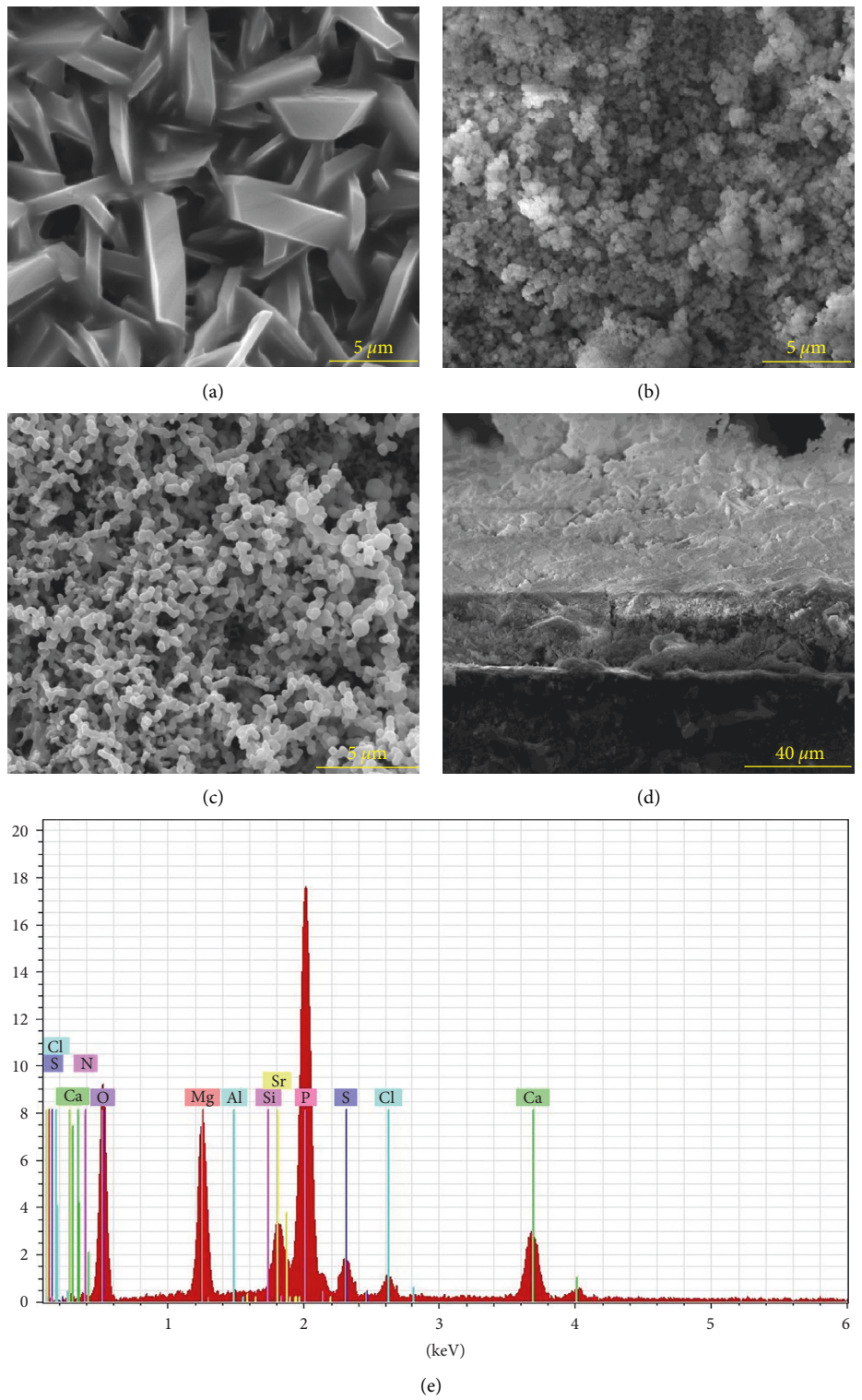

Figure 4: HRSEM micrographs of (a) PEDOT-HNT coated on the Ti alloy, (b) CS-MHA coated on the Ti alloy, (c) PEDOT-HNT/CS-MHA bilayer composite coated on the Ti alloy, (d) cross-sectional image for PEDOT–HNT/CS-MHAP bilayer coating, and (e) EDAX spectrum of the PEDOT-HNT/CS-MHA bilayer composite coated on the Ti alloy.

which shows still higher value than that of the uncoated Ti alloy and PEDOT-HNT-coated Ti alloy samples. The Nyquist plot of bilayer composite coating consists of two semicircles. Where, the semicircle at higher frequencies can be attributed to the PEDOT-HNT/CS-MHA layer and the semicircle at low frequencies to the compact PEDOT-HNT layer. The higher value of Rp for this bilayer composite coating is due to the more effective barrier of the PEDOT-HNT layer

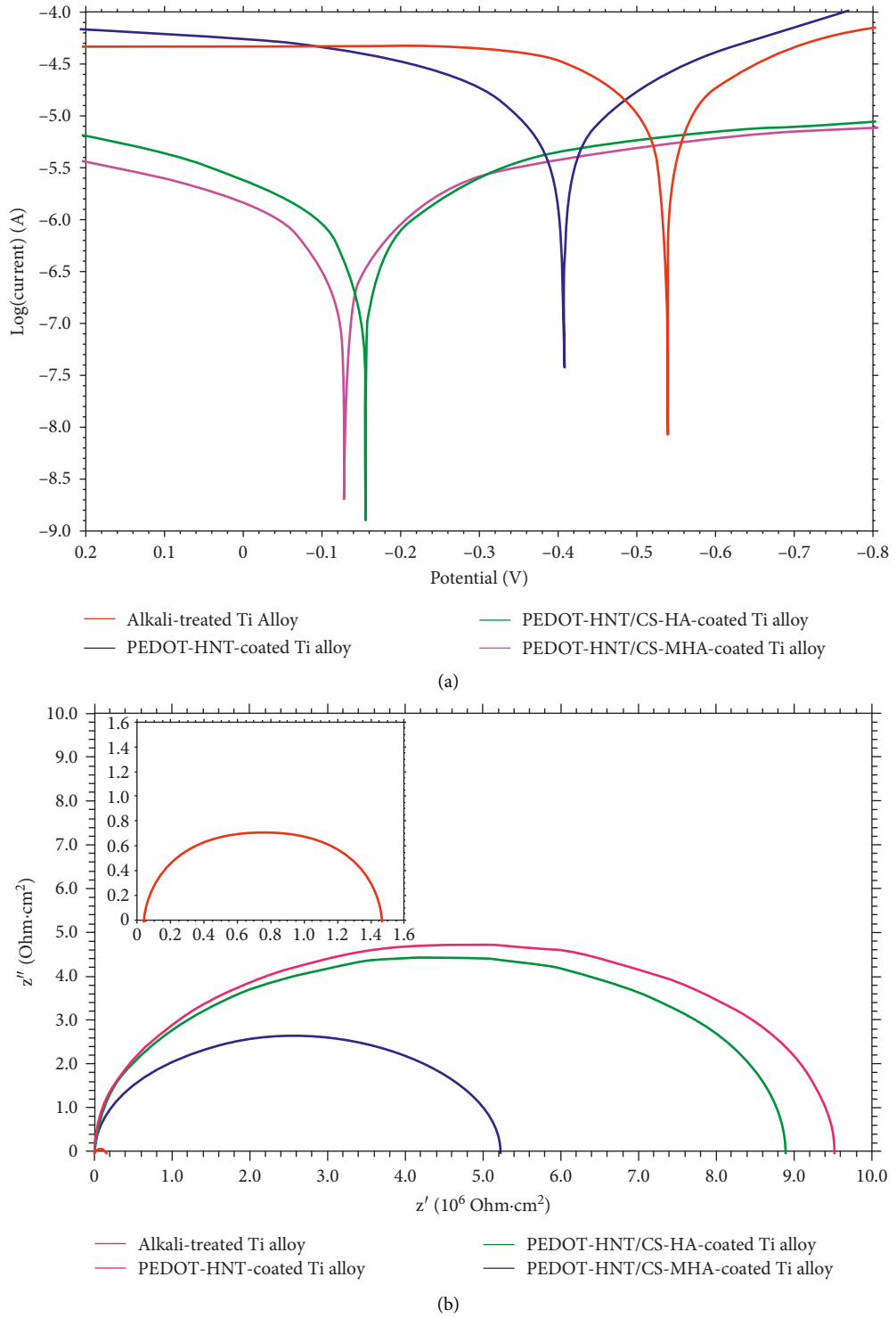

Figure 5: (a) Potentiodynamic polarisation curves of alkali-treated Ti alloy, PEDOT-HNT coated on the Ti alloy, PEDOT-HNT/CS-HA coated on the Ti alloy, and PEDOT-HNT/CS-MHA coated on the Ti alloy in SBF solution. (b) Nyquist plots of alkali-treated Ti alloy, PEDOT-HNT coated on the Ti alloy, PEDOT-HNT/CS-HA coated on the Ti alloy, and PEDOT-HNT/CS-MHA coated on the Ti alloy in SBF solution.

with an underneath passive film and the top-coated PEDOT-HNT/CS-MHA layer. From the above results, it could be well ascertained that the bilayer composite of PEDOT-HNT/CS-MHA on the Ti alloy is superior in corrosion protection.

3.7. Contact Angle Measurements. The wetting contact angle measurements can be described by measuring the optical contact angle (θ).When $\theta = 0$ is complete wetting, $\theta > 90^{\circ}$ is nonwetting (hydrophobic), and $0 < \theta < 90^{\circ}$ is partial wetting

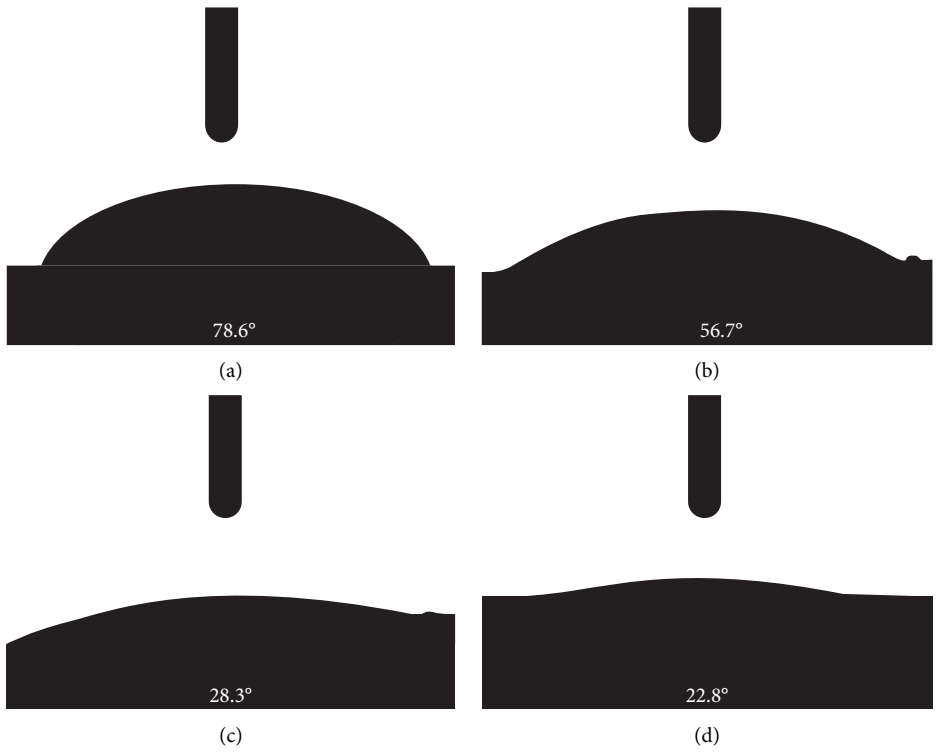

Figure 6: Contact angle measurement of (a) the alkali-treated Ti alloy, (b) PEDOT-HNT composite-coated Ti alloy, and (c) PEDOT-HNT/CS-HA and (d) PEDOT-HNT/CS-MHA bilayer composite-coated Ti alloy. *In vitro* biological studies of the bilayer coating.

(hydrophilic), Figures 6(a)–6(d) show the optical contact angle for the alkali-treated Ti alloy, PEDOT-HNT composite-coated Ti alloy, and PEDOT-HNT/CS-HA and PEDOT-HNT/CS-MHA bilayer composite-coated Ti alloy. It is clearly evident that the surface of the bilayer composite coated on the Ti alloy is most superhydrophilic in comparison to other samples. A linear fit of the contact angle with respect to the thickness is shown in Figures 6(a)–6(d). It shows that the contact angle increases with the increase in the bilayer composite thickness implying the increase of hydrophobic with the increase in thickness. The wettability is an important property of implant materials because the human osteoblast adhesion (CCK-8 assays) and proliferation of the cells are generally better on hydrophilic surfaces. PEDOT-HNT/CS-MHA samples have an excellent hydrophilic surface, whereas their contact angle is less than 90°.

3.8. In Vitro Biological Studies of the Bilayer Coating

3.8.1. Antibacterial Assay. The antibacterial activity of PEDOT-HNT/CS-MHA bilayer composite was studied against Gram-positive *Staphylococcus aureus* and Gram-negative *Escherichia coli* bacterium by the agar well method. The culture medium was incubated with different concentrations of PEDOT-HNT/CS-MHA composite (20 μl, 40 μl, 60 μl, and 80 μl) at 37 °C for 24 h (Figure 7). When increasing the concentration of PEDOT-HNT/CS-MHA, the zone of inhibition values also increase. Subsequently, further increasing the composite concentration ranges of 20 μl, 40 μl, 60 μl, and 80 μl are represented in Table 1. These results indicated PEDOT-HNT/CS-MHA consisting effective antibacterial activity against Gram-positive *Staphylococcus aureus* and Gram-negative *Escherichia coli*. CS-based biomaterials antimicrobial activity has been recently reported. There are several reports on CS enhancing a large number of high chemical reactive amine groups and hydroxyl groups of glucose units, and the flexible structure of the polymer composite elucidated bacterial adhesion on the implant's surface showing antibacterial ability [27-28].

The antibacterial activity of PEDOT-HNT/CS-MHA composite was improved due to the surface of CS on its composite, which could destruct the cell walls of bacteria's. The excellent and broad antibacterial activities of the PEDOT-HNT/CS-MHA composite against both Gram-negative and Gram-positive bacteria indicated that the composite was more suitable for bone defect of infection.

3.9. Cell Viability Test with MG-63 Cells. The cell viability of the PEDOT-HNT/CS-MHA composite coated implant was evaluated on MG-63 osteoblastic cells by the CCK-8 assay. In Figure 8, the cell viability of MG-63 was calculated at different intervals 1, 3, and 7 days. When compared with normal culture cells, the cell viability on the PEDOT-HNT/CS-MHA was significantly higher at days 3 and 7, which suggested that the PEDOT-HNT/CS-MHA enhanced the proliferation of the MG-63 osteoblastic cells. In Figure 8, the phase-contrast microscopic images reveal that, at different time intervals (control and 1, 3, and 7 days), when culture cells with PEDOT-HNT/CS-MHA incubated cells

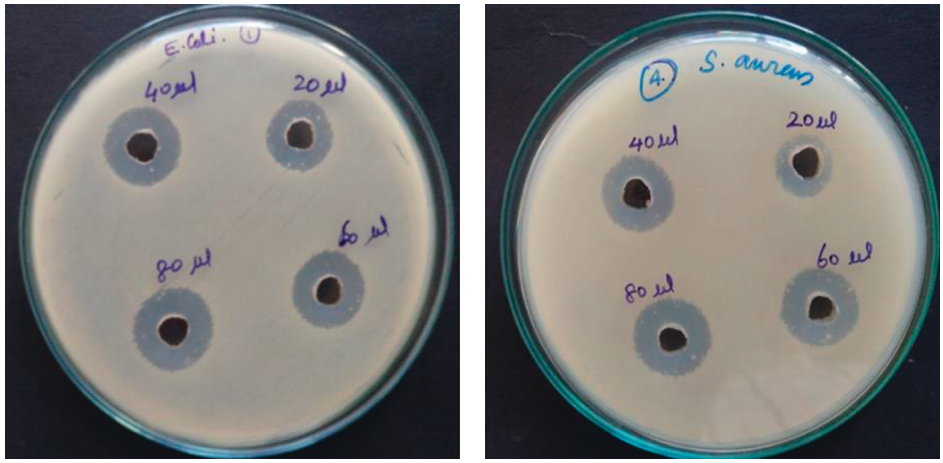

(a) (b)

Figure 7: Antibacterial activity of the PEDOT-HNT/CS-MHA bilayer composite coating against (a) *E. coli* and (b) *S. aureus* bacteria.

Table 1: Antibacterial activity assay.

Name of the bacteria	Zone of inhibition (mm)			
μl of sample	20 μl	40 μl	60 μl	80 μl
Escherichia coli	13	16	17	22
Staphylococcus aureus	12	15	16	18

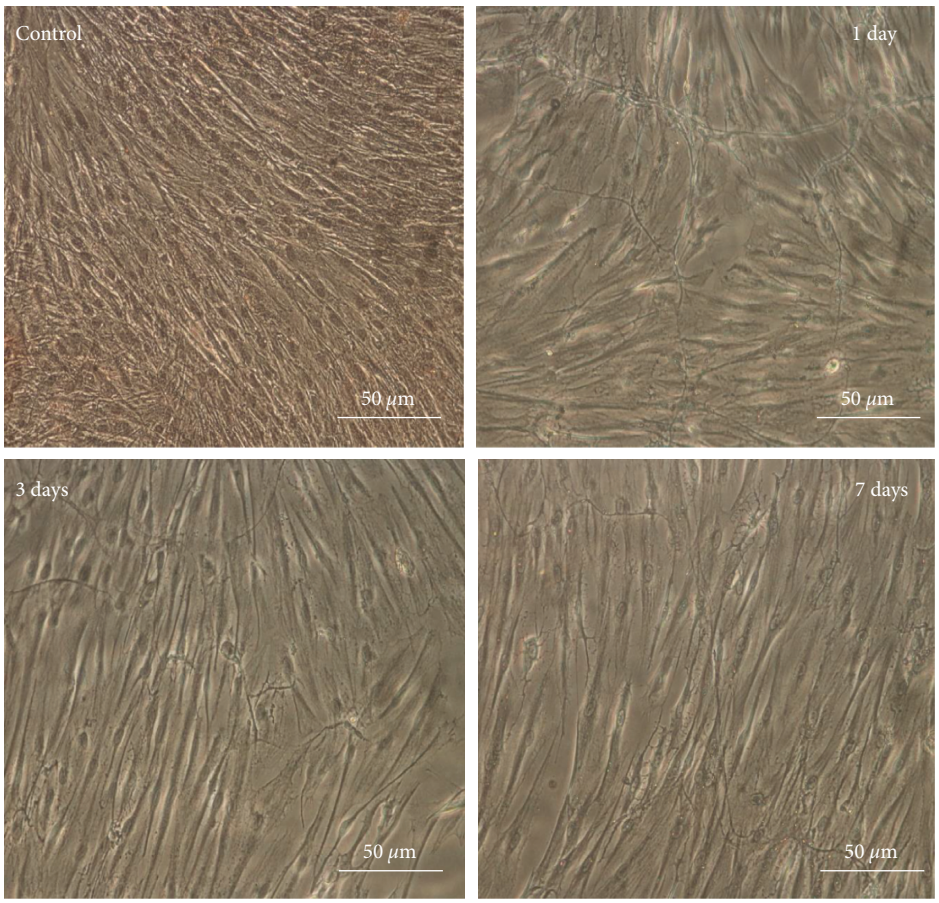

Figure 8: Optical images of the MG-63 cells cultured on the PEDOT-HNT/CS-MHA bilayer-coated implant.

were inserted, PEDOT-HNT/CS-MHA-induced osteoblastic proliferation and differentiation in the bone damaged region. Mg and Sr promote bone formation, and it acted both on osteoblast and osteoclast [25]. Hence, the PEDOT-HNT/CS-MHA-coated Ti alloys show good biocompatibility with MG-63 osteoblastic cells.

4. Conclusion

Alkali-treated Ti alloys, through modification of the physical microstructure of the surface, had a beneficial effect on the corrosion inhibitor and, thus, cell viability to the material. The following points are evident for the PEDOT-HNT/CS-MHA bilayer composites. Moreover, the FTIR, XRD, and spectroscopic results confirm the formation of the composite on Ti alloy samples. Further, the HRSEM results clearly show that uniform and homogeneous PEDOT-HNT/CS-MHA composite coatings were successfully fabricated onto the alkali-treated Ti alloy via the electrodeposition method. The PEDOT-HNT/CS-MHA composite coatings exhibited a bilayer structure, an inner layer consisted of flake-like structure, and an outer layer composed of the spherical-like structure. A significant potential to increase biological activity is also in the modification of the alkali-treated Ti alloy surface of a PEDOT-HNT/CS-MHA bilayer composites material to increase the surface hydrophilicity. The cell experiments suggested significantly increased cell numbers on the alkali-treated Ti alloy. There were more elongated MG-63 cells on the Ti alloy sample in the 7 days culture. In summary, the PEDOT-HNT/CS-MHA bilayer composite coatings might be promising for the surface treatment of Ti which exhibits good corrosion resistance and surface biocompatibility.

Data Availability

The data used to support the findings of this study are available from the corresponding author upon request.

Conflicts of Interest

The authors declare that they have no conflicts of interest.

Acknowledgments

Rangappan Rajavel acknowledges the major financial support from the Council of Scientific and Industrial Research, New Delhi, India (CSIR) (01(2835)/15/EMR-II).

Supplementary Materials

The PEDOT-HNT/CS-MHA composite coatings exhibited a bilayer structure, and an inner layer consisted of flake-like structure, and an outer layer composed of the spherical-like structure. A significant potential to increase biological activity is also in the modification of the alkali-treated Ti alloy surface of a PEDOT-HNT/CS-MHA bilayer composites material to increase the surface hydrophilicity. The composite coatings might be promising for the surface treatment of the Ti alloy which exhibits good corrosion resistance and surface biocompatibility. (*Supplementary Materials*)

References

[1] F. G. Correa, J. V. Granados, M. J. Reyes, and L. A. Q. Granados, "Adsorption behaviour of La(III) and Eu (III) ions from aqueous solutions by hydroxyapatite: kinetic, isotherm, and thermodynamic studies," *Journal of Chemistry*, vol. 2013, Article ID 751696, 9 pages, 2013.

[2] Y. Kirmanidou, M. Sidira, M. E. Drosou et al., "New Ti-alloys and surface modifications to improve the mechanical properties and the biological response to orthopedic and dental implants," *BioMed Research International*, vol. 2016, Article ID 2908570, 21 pages, 2016.

[3] M. Nazir, O. Pei Ting, T. S. Yee, S. Pushparajan, D. Swaminathan, and M. G. Kutty, "Biomimetic coating of modified titanium surfaces with hydroxyapatite using simulated body fluid," *Advances in Materials Science and Engineering*, vol. 2015, Article ID 407379, 8 pages, 2015.

[4] S. L. Assis, S. Wolynec, and I. Costa, "Corrosion characterization of titanium alloys by electrochemical techniques," *Electrochimica Acta*, vol. 51, no. 8-9, pp. 1815–1819, 2006.

[5] Y. Huang, S. Han, X. Pang, Q. Ding, and Y. Yan, "Electrodeposition of porous hydroxyapatite/calcium silicate composite coating on titanium for biomedical applications," *Applied Surface Science*, vol. 271, pp. 299–302, 2013.

[6] N. Pramanik, D. Mishra, I. Banerjee, T. K. Maiti, P. Bhargava, and P. Pramanik, "Chemical synthesis, characterization, and biocompatibility study of hydroxyapatite/chitosan phosphate nanocomposite for bone tissue engineering applications," *International Journal of Biomaterials*, vol. 2009, Article ID 512417, 8 pages, 2009.

[7] N. Murugan, M. Chozhanathmisra, S. Sathishkumar, P. Karthikeyan, and R. Rajavel, "Novel graphene-based reinforced hydroxyapatite composite coatings on titanium with enhanced anti-bacterial, anti-corrosive and biocompatible properties for improved orthopedic applications," *International Journal of Pharmacy and Biological Sciences*, vol. 6, no. 3, pp. 432–442, 2016.

[8] S. L. Aktug, S. Durdu, E. Yalcın, K. Cavusoglu, and M. Usta, "Bioactivity and biocompatibility of hydroxyapatite-based bioceramic coatings on zirconium by plasma electrolytic oxidation," *Materials Science and Engineering: C*, vol. 71, pp. 1020–1027, 2017.

[9] Y. Yajing, D. Qiongqiong, H. Yong, S. Han, and X. Pang, "Magnesium substituted hydroxyapatite coating on titanium with nanotublar TiO_2 intermediate layer via electrochemical deposition," *Applied Surface Science*, vol. 305, pp. 77–85, 2014.

[10] T. Kokubo and H. Takadama, "How useful is SBF in predicting in vivo bone bioactivity," *Biomaterials*, vol. 27, no. 15, pp. 2907–2915, 2006.

[11] G. Fabregat, B. T. Dias, L. J. Valle, E. Armelin, F. Estrany, and C. Aleman, "Incorporation of a clot-binding peptide into polythiophene: properties of composites for biomedical applications," *ACS Applied Materials & Interfaces*, vol. 6, no. 15, pp. 11940–11954, 2014.

[12] S. C. Luo, E. M. Ali, N. C. Tansil et al., "Poly(3, 4-ethylenedioxythiophene) (PEDOT) nanobiointerfaces: thin, ultrasmooth, and functionalized PEDOT films with in vitro and in vivo biocompatibility," *Langmuir*, vol. 24, no. 15, pp. 8071–8077, 2008.

[13] R. F. Vreeland, C. W. Atcherley, W. S. Russell et al., "Biocompatible PEDOT: nafion composite electrode coatings for

selective detection of neurotransmitters in vivo," *Analytical Chemistry*, vol. 87, no. 5, pp. 2600–2607, 2015.

[14] A. M. Kumar, M. A. Hussein, A. Y. Adesina, S. Ramakrishna, and N. A. Aqeeli, "Influence of surface treatment on PEDOT coatings: surface and electrochemical corrosion aspects of newly developed Ti alloy," *RSC Advances*, vol. 8, no. 34, pp. 19181–19195, 2018.

[15] X. Xiong, Y. Wang, W. Zou, J. Duan, and Y. Chen, "Preparation and Characterization of Magnetic Chitosan Microcapsules," *Journal of Chemistry*, vol. 2012, pp. 1–6, 2013.

[16] R. M. Jin, N. Sultana, S. Baba, S. Hamdan, and A. F. Ismail, "Porous PCL/chitosan and nHA/PCL/chitosan scaffolds for tissue engineering applications: fabrication and evaluation," *Journal of Nanomaterials*, vol. 2015, Article ID 357372, 8 pages, 2015.

[17] A. Molaei and M. Yousefpour, "Electrophoretic deposition of chitosan–bioglass–hydroxyapatite–halloysite nanotube composite coating," *Rare Metals*, pp. 1–8, 2018.

[18] M. F. Rada, A. Fatehb, and T. Shahrabi, "Electrophoretic deposition of vancomycin loaded halloysite nanotubes chitosan nanocomposite coatings," *Surface & Coatings Technology*, vol. 349, pp. 144–156, 2018.

[19] G. Cavallaro, G. Lazzara, S. Milioto et al., "Nanohydrogel formation within the halloysite lumen for triggered and sustained release," *ACS Applied Materials & Interfaces*, vol. 10, no. 9, pp. 8265–8273, 2018.

[20] I. Deen and I. Zhitomirsky, "Electrophoretic deposition of composite halloysite nanotube–hydroxyapatite–hyaluronic acid films," *Journal of Alloys and Compounds*, vol. 586, pp. S531–S534, 2014.

[21] G. Cavallaro, D. I. Donato, G. Lazzara, and S. Milioto, "Films of halloysite nanotubes sandwiched between two layers of biopolymer: from the morphology to the dielectric, thermal, transparency, and wettability properties," *Journal of Physical Chemistry C*, vol. 115, no. 42, pp. 20491–20498, 2011.

[22] A. R. Aburto, I. A. G. Saucedo, F. E. Magana et al., "Intercalation of poly(3,4-ethylenedioxythiophene) within halloysite nanotubes: synthesis of composites with improved thermal and electrical properties," *Microporous and Mesoporous Materials*, vol. 218, pp. 118–129, 2015.

[23] G. Renaudin, P. Laquerriere, Y. Filinchuk, and E. J. J. M. Nedelec, "Structural characterization of sol–gel derived Sr-substituted calcium phosphates with anti-osteoporotic and anti-inflammatory properties," *Journal of Materials Chemistry*, vol. 18, no. 30, pp. 3593–3600, 2008.

[24] Y. Li, G. Feng, Y. Gao, E. Luo, X. Liu, and J. Hu, "Strontium ranelate treatment enhances hydroxyapatite-coated titanium screws fixation in osteoporotic rats," *Journal of Orthopaedic Research*, vol. 28, pp. 578–582, 2010.

[25] D. Govindaraj, M. Rajan, M. A. Munusamy, and A. Higuchi, "Mineral substituted hydroxyapatite coatings deposited on nanoporous TiO_2 modulate the directional growth and activity of osteoblastic cells," *RSC Advances*, vol. 5, no. 73, pp. 58980–58988, 2015.

[26] P. Karthikeyan, L. Mitu, K. Pandian, G. Anbarasua, and R. Rajavel, "Electrochemical deposition of a Zn-HNT/p (EDOT-co-EDOP) nanocomposite on LN SS for antibacterial and anti-corrosive applications," *New Journal of Chemistry*, vol. 41, no. 12, pp. 4758–4762, 2017.

[27] A. Chetouani, N. Follain, S. Marais et al., "Physicochemical properties and biological activities of novel blend films using oxidized pectin/chitosan," *International Journal of Biological Macromolecules*, vol. 97, pp. 348–356, 2017.

[28] F. A. Al Sagheer, E. I. Ibrahim, and K. D. Khalil, "Crystallinity, antimicrobial activity and dyeing properties of chitosan-g-poly(*N*-acryloyl morpholine) copolymer," *European Polymer Journal*, vol. 58, pp. 164–172, 2014.